RMJ Ramathibodi Medical Journal

Rama Med J | Original Article

Distinguishing Renal Cell Carcinoma From Other Focal Renal Lesions on Multidetector Computed Tomography

Pornphan Wibulpolprasert[1], Chompoonuch Thongthong[1], Bussanee Wibulpolprasert[1]

[1] Department of Diagnostic and Therapeutic Radiology, Faculty of Medicine Ramathibodi Hospital, Mahidol University, Bangkok, Thailand

Background: The increased use of imaging modalities has led to a greater incidence in depicting solid renal mass. These lesions comprise a wide spectrum of malignant such as renal cell carcinoma (RCC) and benign histologies.

Objective: To determine the multidetector computed tomography (MDCT) features that discriminate RCC from other focal renal lesions.

Methods: A retrospective review was performed on 148 patients who underwent renal CT scan followed by renal surgery or biopsy during January 2008 to July 2014. Specific predictive MDCT features of RCC were determined by logistic regression analysis. Interobserver agreement (kappa [κ] values) was also calculated for each CT feature.

Results: In 148 pathologic proved focal renal lesions, 91 (61.5%) were RCCs and 57 (38.5%) were non-RCCs. RCCs were more likely to be in male patients (OR, 5.39; 95% CI, 2.25 - 12.90), no internal fat component (OR, 46.50; 95% CI, 5.25 - 411.90), locate at peripheral (OR, 7.41; 95% CI, 1.63 - 33.73), and mixed central-peripheral locations (OR, 26.22; 95% CI, 4.23 - 162.58) of the kidney. There was moderate-to-excellent agreement among the readers over all these features (κ = 0.43 - 0.91).

Conclusions: Focal renal lesion with no internal fat component in MDCT is the most useful characteristic in differentiating RCCs from others.

Keywords: Renal cell carcinoma, Renal mass, Computed tomography

Rama Med J: doi:10.33165/rmj.2020.43.1.176267

Received: May 22, 2019 **Revised:** October 29, 2019 **Accepted:** February 6, 2020

Corresponding Author:
Pornphan Wibulpolprasert
Department of Diagnostic and Therapeutic Radiology,
Faculty of Medicine
Ramathibodi Hospital,
Mahidol University,
270 Rama IV Road, Ratchathewi,
Bangkok 10400, Thailand.
Telephone: +66 2201 1212
Fax: +66 2201 1297
E-mail: punlee77@gmail.com,
pornphan.wib@mahidol.ac.th

Introduction

Renal cancer represents around 3% of all cancers with an age-standardized rate (ASR) incidence and mortality per 100 000 of 11.8; 4.1 vs 2.5; 1.3 in males in more developed vs less developed areas and of 5.8; 1.7 vs 1.4; 0.8 in females in more developed vs less developed areas, respectively.[1] Generally, during the last 2 decades, there has been an annual increase of about 2% in the incidence both worldwide and in Europe.[2]

Renal cell carcinoma (RCC) is the most common solid lesion in the kidney and accounts for approximately 90% of all kidney malignancies.[3] In Ramathibodi cancer registry reported in 2014, RCC was found in 42 patients from a total of 54 kidney tumors (77.78%).[4] As tumors are detected more frequently using imaging techniques such as ultrasound, computed tomography (CT), and magnetic resonance imaging (MRI), the numbers of RCC diagnosed incidentally has increased. These tumors are often smaller and at a lower stage than discovered non-incidentally group.[5, 6]

Consequently, the incidence of benign renal masses increases along with incidence of RCC as well as current imaging and biopsy techniques cannot accurately predict the histological features of renal tumors.[7-9] The ball-versus-bean strategy is a useful framework for analyzing the imaging characteristics of renal masses, in which RCC is the prototypic ball-type lesion.[10]

Furthermore, different MDCT features enable to discriminate various renal pathologies. The recent study[11] determined 5 significant MDCT features that can discriminate infiltrative transitional cell carcinomas from other infiltrative renal lesions including solitary lesion, absence of internal calcifications, poor enhancement, presence of pelvicalyceal system involvement and perinephric tissue invasion.

The objectives of this study were to determine the MDCT features that discriminate RCCs from other focal renal lesions by using renal pathology as reference standard.

Methods

Participants and Ethics

The local institutional review board approved this retrospective cross-sectional study (No. MURA2013/307 on May 21, 2013) as following ethical rules. For this type of study formal consent is not required.

This study included images from examinations that were performed with MDCT of the kidney at Ramathibodi Hospital, Mahidol University, Thailand from January 2008 to July 2014. Two last year radiology residents reviewed the report of all CT scans, using "renal mass" as a keyword to select the patients.

The inclusion criteria were imaging diagnosis of focal renal lesion, available imaging of CT scan of the kidney, and undergoing renal surgery with pathology report. Patients with renal cysts (Bosniak classification of I to IIF) and age less than 15 years were excluded.

Study Design

Histopathology Findings

This study reviewed the pathology reports using 2004 WHO histological classification of tumors of the kidney which served as the reference standard for diagnosis of diseases. The surgical specimens from nephrectomy, nephroureterectomy, biopsy, and excision were analyzed by the pathologists.

MDCT

Three MDCT machines were used for all imaging studies according to the standard protocol of the local institution as follows: 1) 320 slices MDCT (Aquilion ONE; Toshiba Medical Systems Corp, Tokyo, Japan; 2) 128 slices MDCT (Aquilion CX; Toshiba Medical Systems Corp, Tokyo, Japan); 3) 64 slice MDCT (SOMATOM Sensation 64; Siemens Medical Solutions, Malvern, PA, USA).

All CT examinations were obtained during patient breath-holding with the following parameters for imaging acquisition and reconstruction: 120 kVp, automated tube current, a section thickness interval of 3 mm, section collimation 0.5 × 80 mm, rotation time 0.5 seconds, pitch factor 0.813, and helical pitch 65. Protocols varied

depending on the type of examination. All patients received about 1000 mL of oral suspension (1000 mL of water and 20 mL contrast material 30 - 60 min before CT and 1.5 - 2 mL/kg (maximum 100 mL) of nonionic 300 - 320 mgI of intravenous (IV) contrast material. The IV contrast material was injected into antecubital vein using a mechanical injector at a rate of 2.5 - 3.0 mL/sec, a bolus tracking algorithm was used to determine the onset of imaging of corticomedullary or arterial phase (30 - 40 seconds), nephrographic or venous phase (70 - 90 seconds). For bolus tracking, a region of interest (ROI) was placed in the thoracoabdominal aorta junction, with a trigger set to begin at 120 - 150 Hounsfield units (HU).

Imaging Interpretation

The MDCT images were independently interpreted by one last year radiology resident and one experienced abdominal imaging radiologist. Each reader used a standardized form to look for imaging features of focal renal lesions. Primary clinical outcome was used to define the imaging features to differentiate RCC from other pathologies.

The CT features in this study were determined as follows: 1) Fatty component: an attenuation threshold of less than or equal to -10 HU with an ROI of at least 19 - 24 mm^2 is optimal for the diagnosis of fat containing angiomyolipoma (AML);[12] 2) Pre-contrast density: the attenuation of the renal parenchyma typically ranges from 30 HU to 40 HU, and that of hyperattenuating renal masses is usually is at least 40 HU, but no higher than 90 HU;[13] 3) Degree of enhancement: the cutoff points to separate tumors into mild, moderate, or avid enhancement groups were 97 HU and 140 HU during the parenchymal phase (70 - 90 seconds after contrast administration), respectively.[14] This study measured the attenuation of a round or elliptical ROI cursor over an enhanced area, which was at least 1 cm^2 and excluded the area of calcification;[15] 4) Three patterns of enhancement: homogenous enhancement is indicated when most areas in the tumor showed a uniform degree of enhancement. Predominantly peripheral enhancement is considered when most portions of the tumor are not enhanced and only the peripheral rim or septa shows enhancement. The remaining cases were considered to have heterogeneous enhancement. The enhancement pattern of a tumor was generally affected by its size because the larger a tumor grows, the more frequently intratumoral necrosis or hemorrhage occurs;[15] 5) Intratumoral vessels: data were recorded when the vessel run into the tumor in post contrast phase scan; 6) Border: the lesions with well-defined border were depicted, which some of them had pseudocapsule, a thin linear enhanced rim/band on post-contrast surrounding the tumor;[16] 7) Location: a centrally located renal tumor is defined as a mass that reaches up to the renal pelvis as opposed to a peripheral renal tumor that protrudes into the perirenal fat.[17] The large tumor reached up to renal pelvis and also protruded into perinephric fat, defining as mixed central and peripheral locating mass; and 8) Associated findings: vascular involvement was defined as irregularities, intraluminal thrombus or enhancement of the renal artery, renal vein or inferior vena cava (IVC). Pelvicalyceal system involvement was defined as filling defect or mural thickening. Perilesional lymphadenopathy was defined as short axis dimension of lymph node measuring more than 1 cm. Adjacent organ involvement was defined as ipsilateral adrenal gland or psoas muscle involvement. Perinephric fat involvement was defined as perinephric fat stranding or soft tissue extension from the mass. Distant metastasis was defined as lung, mediastinal, bone or liver involvement.

Statistical Analysis

Interobserver agreement was assessed by kappa (κ) analysis.[18] A κ value of less than 0.20 indicated poor agreement; 0.21 - 0.40, fair agreement; 0.41 - 0.60, moderate agreement; 0.61 - 0.80, good agreement; and 0.81 - 1.00, excellent agreement.

Comparatively categorical variables of imaging features were tested by chi-square test or Fisher exact test, and comparatively continuous variables of imaging features were tested by *t* test or Mann-Whitney test.

Predictive factors of RCC and malignancy were determined by logistic regression analysis. The results

were expressed as odds ratio (OR), 95% confidence interval (CI), and *P* value. After a number of univariate predictive factors had been determined, forward stepwise selection was carried out to determine the appropriate multivariate model. Factors selected for the multivariate model were those found significant in the univariate model.

All statistical analyses were performed by using STATA version 13 (Stata Corp. Version 13. College Station, TX: StataCorp LP; 2013). A *P* value of less than .05 was considered statistically significant.

Results

Clinicopathological Characteristics of Patients

This study included 148 pathologically proven focal renal lesions detected on CT in 148 patients. The population was stratified into 2 groups based on the final histopathological diagnosis from surgery. One group with 91 lesions (61.5%) were diagnosed as RCCs and another group with 57 lesions (38.5%) were diagnosed as non-RCCs, compose of benign and other malignant lesions. The mean (standard deviation, SD) age of the patients with RCCs was 59.0 (13.3) years and for the patients with non-RCCs was 54.6 (12.8) years. There was no statistically significant difference between 2 groups ($P = .05$). Among 64 patients with RCCs (70.3%) were male whereas 42 patients with non-RCCs (73.7%) were female. There was statistically significant difference between 2 groups ($P < .001$). For the presenting symptoms, gross hematuria was found in 10 RCCs and 4 non-RCCs. Flank pain (ipsilateral) was found in 1 RCC and 4 non-RCCs. Palpable mass was found in 4 RCCs and 2 non-RCCs. Weight loss or severe fatigue was found in 1 RCC. There was no statistically significant difference of presenting symptoms between these 2 groups. The median (range) of tumor size was 6.2 (1.4 - 25.0) cm for RCCs and 5.7 (1.1 - 27.0) cm for non-RCCs ($P = .80$) (Table 1).

Table 1. Clinicopathological Characteristics of Patients

Parameter	No. (%)			*P* Value*
	Total (N = 148)	RCCs (n = 91)	Non-RCCs (n = 57)	
Age, mean (SD), y	57.3 (13.3)	59.0 (13.3)	54.6 (12.8)	.05
Gender				
Male	79 (53.4)	64 (70.3)	15 (26.3)	< .001
Female	69 (46.6)	27 (29.7)	42 (73.7)	
Presenting symptoms				
Gross hematuria	14 (9.5)	10 (11.0)	4 (7.0)	.42
Flank pain (ipsilateral)	5 (3.4)	1 (1.1)	4 (7.0)	.07
Palpable mass	6 (4.1)	4 (4.4)	2 (3.5)	1.00
Weight loss or severe fatigue	1 (0.7)	1 (1.1)	0 (0)	1.00
Asymptomatic	2 (1.4)	1 (1.1)	1 (1.8)	1.00
No history	16 (10.8)	9 (9.9)	7 (12.9)	.65
Others	104 (70.3)	65 (71.4)	39 (69.6)	.50
Tumor size, median (range), cm	6.0 (1.1 - 7.0)	6.2 (1.4 - 25.0)	5.7 (1.1 - 27.0)	.80

Abbreviations: RCC, renal cell carcinoma; SD, standard deviation.

* $P < .05$ was considered statistically significant.

Interobserver agreement of calcification, pattern of enhancement, pelvicalyceal involvement, and distant metastasis showed excellent agreement (κ = 0.82 - 0.91). Interobserver agreement of intratumoral vessels, vascular involvement, and perinephric fat involvement showed good agreement (κ = 0.74 - 0.80). Interobserver agreement of border, location, and adjacent organ involvement showed moderate agreement (κ = 0.43 - 0.59).

Number of RCC and Non-RCC in Focal Renal Lesion From Pathological Findings

Of the overall 148 renal lesions included in this study, 91 (61.5%) were RCCs, and 57 (38.5%) were non-RCCs. Of the 91 RCCs, 64 (70.3%) were clear cell RCCs (Figure 1), 10 (11%) were papillary RCCs, 7 (7.7%) were chromophobe RCCs, 8 (8.8%) were unclassified RCCs, and 2 (2.2%) were mixed subtypes RCCs. The non-RCC lesions were stratified into 2 categories; first group included all of benign lesions such as AML, oncocytoma, metanephric adenoma, xanthogranulomatous pyelonephritis, cystic nephroma, hemangioma, and second group included non-RCC malignant lesions such as TCC, metastasis, and sarcoma (Table 2).

Table 2. Number of RCCs and Non-RCCs in Focal Renal Lesions From Pathological Findings

Diagnosis	No. (%)
RCCs	91 (61.5)
Non-RCCs	57 (38.5)
Benign lesions	41 (27.7)
AML*	27 (18.2)
Oncocytoma	4 (2.7)
Metanephric adenoma	1 (0.7)
Xanthogranulomatous pyelonephritis	1 (0.7)
Cystic nephroma	1 (0.7)
Hemangioma	2 (1.4)
Other benign lesions	5 (3.4)
Malignancy	16 (10.8)
TCCs	7 (4.7)
Metastasis	5 (3.4)
Sarcoma	3 (2.0)
Other malignant lesions	1 (0.7)

Abbreviations: AML, angiomyolipoma; RCCs, renal cell carcinomas; TCCs, transitional cell carcinomas.

*Nonfat-containing AML 8 lesions.

Figure 1. Computed Tomography (CT) Feature of Clear Cell Renal Cell Carcinoma in the Right Kidney of a 49-Year-Old Male Who Presented With Gross Hematuria

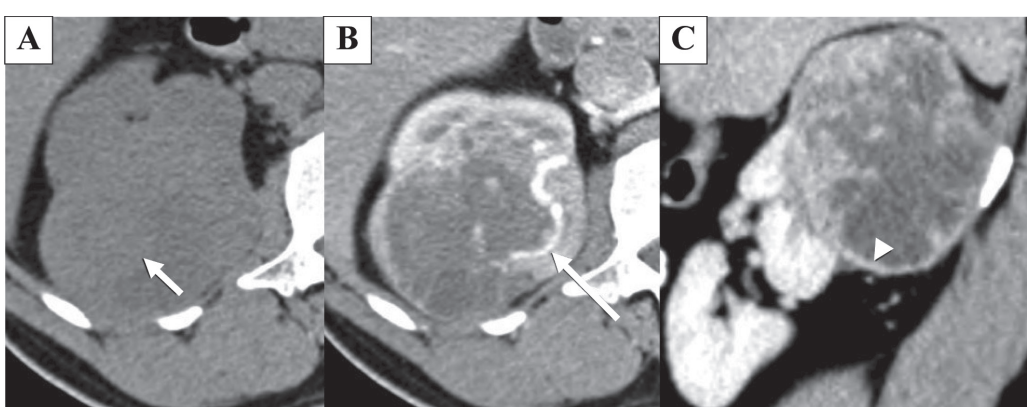

Axial non-enhanced MDCT scan (A) demonstrated an isoattenuated lesion (36 HU) without fat component or calcification (short arrow). Axial contrast-enhanced multidetector computed tomography (MDCT) scan during arterial phase (B) showed intratumoral vessel (arrow). Sagittal contrast-enhanced MDCT scan during venous phase (C) revealed predominantly peripheral and mild enhancement (87 HU) of peripherally locating mass surrounding with pseudocapsule (arrowhead).

Comparison of Imaging Features of RCC vs Non-RCC

Details of imaging features of RCCs vs non-RCCs were compared. The imaging features which showed a statistical difference between RCC and non-RCC included internal fatty component ($P < .001$), border ($P = .008$), tumor location ($P = .01$), vascular involvement ($P = .003$), pelvicalyceal involvement ($P = .007$), and perinephric fat involvement ($P = .003$). The imaging feature which showed a statistical difference between subtypes of RCC was intratumoral vessels ($P = .002$) (Table 3).

Suggestive Features of RCC Compared With Non-RCC in Focal Renal Lesions

Multivariate logistic regression analysis results of the CT image characteristics determined 4 predictive factors of RCC compared with non-RCC consisting of male gender (OR, 5.39; 95% CI, 2.25 - 12.90; $P < .001$), no fatty component (OR, 46.50; 95% CI, 5.25 - 411.90; $P = .001$), peripheral location (OR, 7.41; 95% CI, 1.63 - 33.73; $P = .01$), as well as mixed central and peripheral locations (OR, 26.22; 95% CI, 4.23 - 162.58; $P < .001$).

Suggestive Features of Malignancy Compared With Benign Lesions in Focal Renal Lesions

Multivariate logistic regression analysis results of the CT image characteristics determined 2 predictive factors of malignancy compared with benign focal renal lesions consisting of no fatty component (OR, 45.16; 95% CI, 5.46 - 373.19; $P < .001$) and vascular involvement (OR, 8.08; 95% CI, 1.42 - 46.15; $P = .02$).

Suggestive Features of RCC Compared With AML in Focal Renal Lesions

Multivariate logistic regression analysis results of the CT image characteristics determined 4 predictive factors of RCC compared with AML consisting of solitary lesion (OR, 9.96; 95% CI, 1.31 - 75.76; $P = .03$), isoattenuation on non-contrasted CT (OR, 6.01; 95% CI, 1.42 - 25.46; $P = .02$), pelvicalyceal involvement (OR, 20.89; 95% CI, 2.44 - 178.60; $P = .006$), and perinephric fat involvement (OR, 5.62; 95% CI, 1.37 - 23.05; $P = .02$) (Figure 2).

Table 3. CT Imaging Features of RCCs vs Non-RCCs in Focal Renal Lesions

Feature	No. (%)		*P* Value*
	RCCs (n = 91)	Non-RCCs (n = 57)	
Lesions			
Solitary	87 (95.6)	49 (86.0)	.06
Multiple	4 (4.4)	8 (14.0)	
Calcification			
Peripheral rim	8 (8.8)	6 (10.5)	.39
Non-peripheral	14 (15.4)	5 (8.8)	
Combination	8 (8.8)	2 (3.5)	
None	61 (67.0)	44 (77.2)	
Presence of fatty component	1 (1.1)	19 (33.3)	<.001
Pre-contrast density			
Hyperdense (> 40 HU)	18 (19.8)	19 (33.3)	.06
Isodense (30 - 40 HU)	48 (52.8)	20 (35.1)	
Hypodense (< 30 HU)	24 (26.4)	15 (26.3)	
None	1 (1.10)	3 (5.26)	

Table 3. CT Imaging Features of RCCs vs Non-RCCs in Focal Renal Lesions (Continued)

Feature	No. (%)		*P* Value*
	RCCs (n = 91)	Non-RCCs (n = 57)	
Degree of enhancement			
Mild (< 97 HU)	45 (49.5)	36 (63.2)	.21
Moderate (97 - 140 HU)	39 (42.9)	15 (26.3)	
Avid (> 140 HU)	3 (3.3)	2 (3.5)	
None	4 (4.4)	4 (7.0)	
Enhancement pattern			
Homogeneous	10 (11.0)	14 (24.6)	.12
Heterogeneous	49 (53.9)	27 (47.4)	
Predominantly peripheral	28 (30.8)	13 (22.8)	
Complex cyst	1 (1.1)	2 (3.5)	
None	3 (3.3)	1 (1.8)	
Presence of intratumoral vessels	67 (73.6)	40 (70.2)	.70
Border			
Well-defined	49 (53.9)	43 (75.4)	.008
Pseudocapsule	42 (46.2)	14 (24.6)	
Location			
Central	3 (3.3)	8 (14.0)	.01
Peripheral	61 (67.0)	41 (71.9)	
Mixed central and peripheral	27 (29.7)	8 (14.0)	
Associated findings**			
Vascular involvement	19 (20.9)	2 (3.6)	.003
Pelvicalyceal involvement	48 (52.8)	18 (32.1)	.007
Perilesional lymph node	8 (8.8)	4 (7.0)	.77
Adjacent organ involvement	1 (1.1)	2 (3.5)	.56
Perinephric fat involvement	53 (58.9)	19 (33.3)	.003
Distant metastasis	14 (15.4)	5 (8.8)	.24

Abbreviations: CT, computed tomography; RCC, renal cell carcinoma.

*$P < .05$ was considered statistically significant.

** One lesion might have more than one associated MDCT findings.

Figure 2. Computed tomography (CT) Feature of Multiple Angiomyolipomas (AMLs) in the Right Kidney of a 47-Year-Old Asymptomatic Female

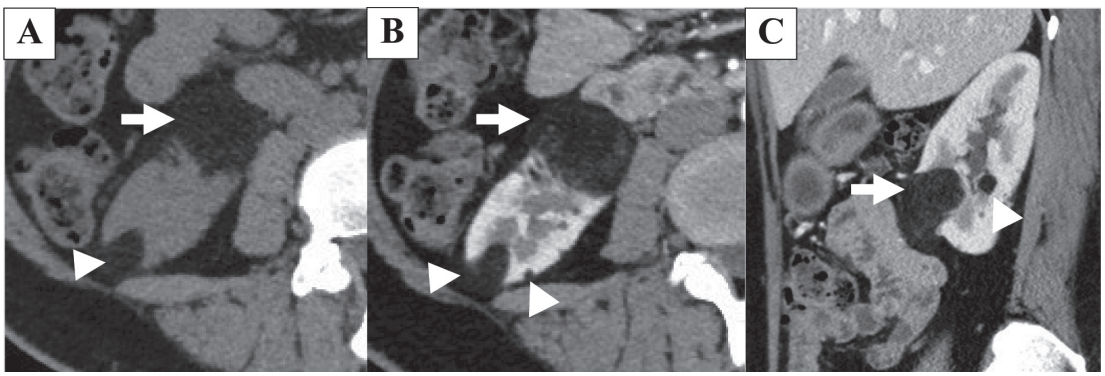

Axial non-enhanced multidetector computed tomography (MDCT) scan (A) demonstrated a fat containing peripheral locating lesion (-50 HU) without calcification (arrow). Axial (B) and sagittal (C) contrast-enhanced MDCT scan showed heterogeneous enhancement. A few smaller lesions with same density and enhancement were demonstrated (short arrow in A, B, and C).

Discussion

CT scan has been widely used for the evaluation of renal tumors because CT can provide detailed tumor information. Furthermore, with the use of helical CT, it is possible to analyze the dynamic enhancement pattern of the tumor, which enables the differentiation of many renal neoplasms.[19]

In this study, the most common pathologic findings of focal renal lesions that underwent surgery was RCC (61.5%) followed by AML (27.7%), and oncocytoma (18.2%). As previously reported,[20] RCCs were classified into clear cell (70.3%), papillary (11%), chromophobe (7.7%), unclassified (8.8%), and mixed subtypes (2.2%). Clear cell RCC was the most common RCC subtype. The occurrence of RCC peaked in the 6th decade of life, with male predominance. Diagnosed RCC may have been discovered incidentally during imaging performed for non-urologic symptoms, which corresponds with previous reports that characterized RCC by a lack of early-warning signs.[10, 21]

With regard to calcification patterns, Dyer et al[10] revealed the presence of centrally located calcification was characteristic of RCC. This result was similar to the present study demonstrating that non-peripheral calcification was more common in RCC (15.4%) than non-RCC (8.8%). However, there was no statistically significant ($P = .39$).

Previous study revealed that the presence of pseudocapsule is recognized in early stage of RCC and usually absent in AML, especially in the case with absence of internal fat component.[22] In the present study, univariate logistic regression analysis revealed that positive predicting factor for RCC compared to non-RCC was the presence of pseudocapsule (OR, 2.63; 95% CI, 1.27 - 5.47), as well as the positive predicting factor for RCC compared to AML was the presence of pseudocapsule (OR, 3; 95% CI, 1.11 - 8.13). This feature may be useful in surgical planning, because the presence of pseudocapsule may make enucleation easier.[23]

A study of Kim et al[24] found that homogeneous enhancement pattern was a valuable CT finding to differentiate AML with minimal fat from RCC, with positive and negative predictive values as high as 91% and 87%, respectively. The present study showed that enhancement pattern was not useful as an indicator to differentiate AML (non-containing fat) from RCC ($P = .27$), which was probably due to small disproportional sample size of 8 nonfat-containing AML vs 91 RCCs.

A fat-containing RCC must be considered when a fat-containing renal tumor is detected, even though the presence of intratumoral fat is characteristic of AML. Malignancy should be suspected when one or more of

the following criteria are present; intratumor calcifications, a large irregular tumor invading perirenal or sinus fat, a large necrotic tumor with small foci of fat, and association with non-fatty lymph nodes or venous invasion.[25] According to the present study, fat containing lesions significantly predicted AML by 95% and RCC by 5%. Only one fat-containing RCC was found in a 67-year-old male came for check-up. However, this mass showed combined central and peripheral calcifications, large size (24 cm), and pelvicalyceal system involvement. However, there were only 2 case reports with similar pattern.[25, 26] The intratumoral foci of fat and calcification were attributed to osseous metaplasia of the nonepithelial stromal portion of the tumor, with growth of fatty marrow elements and trabeculae.[27]

High tumor attenuation on unenhanced scans has been presented as a unique finding in AML with minimal fat in previous reports[28, 29] which was probably due to this AML subtype which consisted mostly of smooth muscle.[13] Kim et al[24] also revealed high tumor attenuation was more common among patients with minimal fat AML (53%), than those with RCC (13%) (P = .04), although the frequency of hypoattenuation or isoattenuation was not statistically significant difference between these 2 diseases (P > .05). This was in contrast with the present study that showed no statistically significant (P = .07) of tumor density on non-enhanced CT scan between nonfat-containing AML and RCC. These results corresponded with a study of Milner et al[30] which showed that not all AML expressed hyperdense on non-enhanced CT and all of AML cannot be reliably identified by imaging.

According to pathophysiology of RCC, the majority of RCCs arise from cells of proximal renal tubular epithelium (lining cell of the proximal convoluted tubule) at the renal cortex. This evidence was supported by the result of this study. Multivariate logistic regression analysis demonstrated that peripheral locating renal lesion and mixed central- peripheral locating renal lesions were the positive predicting factors of RCC (OR, 7.41; 95% CI, 1.63 - 33.73 and OR, 26.22; 95% CI, 4.23 - 162.58, respectively).

The classification of renal cell carcinoma into subtypes has become more interesting because each subtype is associated with different prognosis. Previous published studies[15] have revealed renal attenuation profiles from multiphasic multidetector CT may assist in discrimination of clear cell RCC from other solid cortical renal masses, particularly papillary RCC and lipid poor AML. Clear cell RCC usually showed stronger enhancement than papillary RCC in corticomedullary and nephrographic phases. There were no statistically significant differences in frequency of predominantly peripheral enhancement between clear cell RCC, papillary RCC, and chromophobe RCC (P >.05).[15] The finding of the present study found that the degree of enhancement and enhancement pattern revealed no statistically significant difference between subtypes of RCC with P value of .23 and .12, respectively. The tumor size was also not significantly different among clear cell, papillary, and chromophobe, unclassified, and mix-typed renal carcinoma (P = .40), as seen in the previous report.[15] The major reason for this result was probably due to relative small and disproportional number of cases in each RCC subtypes.

According to the results of the multivariate logistic regression analysis, male, no fatty component, peripheral location, and mixed central-peripheral locations were valuable CT findings for differentiating RCC from non-RCC. No fatty component and vascular involvement were valuable CT findings for differentiating malignant from benign lesions. Moreover, solitary focal renal lesion, isoattenuation on non-contrasted CT, presence of pelvicalyceal system, and perinephric fat involvement were valuable CT findings for differentiating RCC from AML.

Although radiological imaging has been the primary tool to evaluate renal mass lesion, imaging alone may not be able to obviate surgery for all benign renal lesions. Percutaneous biopsy is expected to play a crucial role in determining the optimal management of patients with indeterminate renal lesion. Still, consensus on when and how percutaneous biopsy should be performed for small renal mass will need to be validated in the future.

There are several emerging imaging technologies such as sonoelastrography, diffusion-weighted MRI,

or CT pixel histogram analysis for differentiation of AML which may differentiate the most common benign renal tumor from RCC, but these still need further validation. A growing interpreter experience which emphasizes imaging characteristics of renal mass combined with emerging imaging technologies may help to improve early diagnosis of RCC for the maximum benefit of early treatment outcome and the best prognosis.

There were several limitations in this study. The major limitation was relatively small sample size to analyze CT features. Therefore, further investigation with more adequate numbers of patients will be necessary. Second, this study was a retrospective study, so it has intrinsic selection bias based on the study design. Third, this study was a single-institution experience, and the results may not be widely applicable. Fourth, patients were evaluated with focal renal lesion from CT scan of the patients who underwent renal surgery and excluded patients without pathological proof for focal renal lesion. Therefore, these findings may not reflect the whole population of patients with RCC or other renal cancers.

Despite these limitations, this study is the first, to evaluate the CT characteristics of RCC compared with other focal renal lesions. Furthermore, this study also determined predictive factors of malignancy among Thai patients who underwent renal surgery with renal surgical specimen as the reference standard.

Conclusions

The focal renal lesions with no fatty component was the most valuable CT imaging characteristic for differentiating RCCs from non-RCCs and malignant from benign lesions. Male, peripheral location, and mixed central-peripheral locations played supplementary roles in differentiating RCC from non-RCC lesions.

Acknowledgments

The authors acknowledge Stephen Pinder, a native speaking specialist in medical English, for review and editing of the draft manuscript.

References

1. Jemal A, Bray F, Center MM, Ferlay J, Ward E, Forman D. Global cancer statistics. *CA Cancer J Clin.* 2011; 61(2):69-90. doi:10.3322/caac.20107.
2. Lindblad P. Epidemiology of renal cell carcinoma. *Scand J Surg.* 2004;93(2):88-96. doi:10.1177/145749690409300202.
3. Kovacs G, Akhtar M, Beckwith BJ, et al. The Heidelberg classification of renal cell tumours. *J Pathol.* 1997;183(2):131-133. doi:10.1002/(SICI)1096-9896(199710)183:2<131::AID-PATH931>3.0.CO;2-G.
4. Cancer Registry, Ramathibodi Hospital, Mahidol University. Ramathibodi Cancer Report 2014. http://med.mahidol.ac.th/cancer_center/sites/default/files/public/pdf/Annual_Rama_2014.pdf. Accessed January 6, 2020.
5. Patard JJ, Rodriguez A, Rioux-Leclercq N, Guillé F, Lobel B. Prognostic significance of the mode of detection in renal tumours. *BJU Int.* 2002;90(4):358-363. doi:10.1046/j.1464-410X.2002.02910.x.
6. Kato M, Suzuki T, Suzuki Y, Terasawa Y, Sasano H, Arai Y. Natural history of small renal cell carcinoma: evaluation of growth rate, histological grade, cell proliferation and apoptosis. *J Urol.* 2004;172(3): 863-866. doi:10.1097/01.ju.0000136315.80057.99.
7. Hollingsworth JM, Miller DC, Daignault S, Hollenbeck BK. Rising incidence of small renal masses: a need to reassess treatment effect. *J Natl Cancer Inst.* 2006;98(18): 1331-1334. doi:10.1093/jnci/djj362.
8. Murphy AM, Buck AM, Benson MC, McKiernan JM. Increasing detection rate of benign renal tumors: evaluation of factors predicting for benign tumor histologic features during past two decades. *Urology.* 2009;73(6):1293-1297. doi:10.1016/j.urology.2008.12.072.
9. Silverman SG, Gan YU, Mortele KJ, Tuncali K, Cibas ES. Renal masses in the adult patient: the role of percutaneous biopsy. *Radiology.* 2006;240(1):6-22. doi:10.1148/radiol.2401050061.
10. Dyer R, DiSantis DJ, McClennan

BL. Simplified imaging approach for evaluation of the solid renal mass in adults. *Radiology*. 2008; 247(2):331-343. doi:10.1148/radiol.2472061846.

11. Wibulpolprasert P, Jungtheerapanich S, Wibulpolprasert B. Distinguishing infiltrative transitional cell carcinoma from other infiltrative lesions of the kidneys on multidetector computed tomography. *Rama Med J*. 2019;42(4):1-11. doi:10.14456/rmj.2019.42.4.176646.
12. Davenport MS, Neville AM, Ellis JH, Cohan RH, Chaudhry HS, Leder RA. Diagnosis of renal angiomyolipoma with Hounsfield unit thresholds: effect of size of region of interest and nephrographic phase imaging. *Radiology*. 2011; 260(1):158-165. doi:10.1148/radiol.11102476.
13. Silverman SG, Mortele KJ, Tuncal K, Jinzaki M, Cibas ES. Hyperattenuating renal masses: etiologies, pathogenesis, and imaging evaluation. *Radiographics*. 2007; 27(4):1131-1143. doi:10.1148/rg.274065147.
14. Zhang J, Lefkowitz RA, Ishill NM, et al. Solid renal cortical tumors: differentiation with CT. *Radiology*. 2007;244(2):494-504. doi:10.1148/radiol.2442060927.
15. Kim JK, Kim TK, Ahn HJ, Kim CS, Kim KR, Cho KS. Differentiation of subtypes of renal cell carcinoma on helical CT scans. *AJR Am J Roentgenol*. 2002;178(6):1499-1506. doi:10.2214/ajr.178.6.1781499.
16. Tsili AC, Argyropoulou MI, Gousia A, et al. Renal cell carcinoma: value of multiphase MDCT with multiplanar reformations in the detection of pseudocapsule. *AJR Am J Roentgenol*. 2012;199(2): 379-386. doi:10.2214/AJR.11.7747.
17. Raza SA, Sohaib SA, Sahdev A, et al. Centrally infiltrating renal masses on CT: differentiating intrarenal transitional cell carcinoma from centrally located renal cell carcinoma. *AJR Am J Roentgenol*. 2012;198(4):846-853. doi:10.2214/AJR.11.7376.
18. McHugh ML. Interrater reliability: the kappa statistic. *Biochem Med (Zagreb)*. 2012;22(3):276-282.
19. Zhang YY, Luo S, Liu Y, Xu RT. Angiomyolipoma with minimal fat: differentiation from papillary renal cell carcinoma by helical CT. *Clin Radiol*. 2013;68(4):365-370. doi:10.1016/j.crad.2012.08.028.
20. Prasad SR, Humphrey PA, Catena JR, et al. Common and uncommon histologic subtypes of renal cell carcinoma: imaging spectrum with pathologic correlation. *Radiographics*. 2006; 26(6):1795-1806 doi:10.1148/rg.266065010.
21. Motzer RJ, Bander NH, Nanus DM. Renal-cell carcinoma. *N Engl J Med*. 1996;335(12):865-875. doi:10.1056/NEJM199609193351207.
22. Tsili AC, Argyropoulou MI. Advances of multidetector computed tomography in the characterization and staging of renal cell carcinoma. *World J Radiol*. 2015;7(6):110-127. doi:10.4329/wjr.v7.i6.110.
23. Renal Tumors. In: Dunnick NR, Sandler CM, Newhouse JH, eds. *Textbook of Uroradiology*. 5th ed. Philadelphia: Lippincott Williams & Wilkins; 2013:126-155.
24. Kim JK, Park SY, Shon JH, Cho KS. Angiomyolipoma with minimal fat: differentiation from renal cell carcinoma at biphasic helical CT. *Radiology*. 2004;230(3):677-684. doi:10.1148/radiol.2303030003.
25. Hélénon O, Chrétien Y, Paraf F, Melki P, Denys A, Moreau JF. Renal cell carcinoma containing fat: demonstration with CT. *Radiology*. 1993;188(2):429-430. doi:10.1148/radiology.188.2.8327691.
26. Strotzer M, Lehner KB, Becker K. Detection of fat in a renal cell carcinoma mimicking angiomyolipoma. *Radiology*. 1993;188(2):427-428. doi:10.1148/radiology.188.2.8327690.
27. Hélénon O, Merran S, Paraf F, et al. Unusual fat-containing tumors of the kidney: a diagnostic dilemma. *Radiographics*. 1997;17(1):129-144.
28. Obuz F, Karabay N, Seçil M, İğci E, Kovanlikaya A, Yörükoğlu K. Various radiological appearances of angiomyolipoinas in the same kidney. *Eur Radiol*. 2000;10(6): 897-899. doi:10.1007/s003300051031.
29. Hosokawa Y, Kinouchi T, Sawai Y, et al. Renal angiomyolipoma with minimal fat. *Int J Clin Oncol*. 2002;7(2):120-123. doi:10.1007/s101470200016.
30. Milner J, McNeil B, Alioto J, et al. Fat poor renal angiomyolipoma: patient, computerized tomography and histological findings. *J Urol*. 2006;176(3):905-909. doi:10.1016/j.juro.2006.04.016.

RMJ Ramathibodi Medical Journal

Rama Med J | Original Article

การแยกมะเร็งของไตชนิดเซลล์เนื้อเยื่อไต ออกจากพยาธิสภาพอื่นๆ ของไตที่มีลักษณะเป็นก้อนเดี่ยวจากภาพเอกซเรย์คอมพิวเตอร์

พรพรรณ วิบุลผลประเสริฐ[1], ชมพูนุช ธงทอง[1], บุษณี วิบุลผลประเสริฐ[1]

[1] ภาควิชารังสีวิทยา คณะแพทยศาสตร์โรงพยาบาลรามาธิบดี มหาวิทยาลัยมหิดล กรุงเทพฯ ประเทศไทย

บทนำ: ปัจจุบันมีการใช้เครื่องมือในการตรวจวินิจฉัยทางรังสีเพิ่มขึ้น ส่งผลให้มีการตรวจพบความผิดปกติในร่างกายเพิ่มขึ้น รวมถึงการพบก้อนเนื้อของไตที่อาจมีสาเหตุมาจากเนื้อร้าย ซึ่งชนิดที่พบบ่อยที่สุดคือ มะเร็งไตชนิดเซลล์เนื้อเยื่อไต (Renal cell carcinoma, RCC) หรืออาจเป็นความผิดปกติที่ไม่อันตรายร้ายแรง

วัตถุประสงค์: เพื่อระบุลักษณะภาพเอกซเรย์คอมพิวเตอร์ (Multidetector computed tomography, MDCT) ในการแยกมะเร็งไตชนิดเซลล์เนื้อเยื่อไตออกจากพยาธิสภาพอื่น

วิธีการศึกษา: การศึกษาย้อนหลังจากผู้ป่วยจำนวน 148 คน ที่มีความผิดปกติของไตลักษณะเป็นก้อนเดี่ยวในภาพเอกซเรย์คอมพิวเตอร์ และได้รับการผ่าตัดในช่วงเดือนมกราคม พ.ศ. 2551 ถึงเดือนกรกฎาคม พ.ศ. 2557 ข้อมูลต่างๆ ถูกนำมาเปรียบเทียบระหว่างกลุ่มมะเร็งไตชนิดเซลล์เนื้อเยื่อไต กับกลุ่มโรคอื่นๆ จากนั้นทำการวิเคราะห์โดยใช้สถิติ Logistic regression analysis และประเมินค่าความเชื่อมั่นจากการสังเกต (Interobserver agreement) โดยใช้การวิเคราะห์ Kappa [κ] analysis

ผลการศึกษา: ก้อนของไตจากภาพเอกซเรย์คอมพิวเตอร์ จำนวน 148 ก้อน แบ่งเป็น มะเร็งไตชนิดเซลล์เนื้อเยื่อไต จำนวน 91 ก้อน คิดเป็นร้อยละ 61.5 และจากพยาธิสภาพอื่น จำนวน 57 ก้อน คิดเป็นร้อยละ 38.5 ส่วนใหญ่พบมะเร็งไตชนิดเซลล์เนื้อเยื่อไตในเพศชาย (OR, 5.39; 95% CI, 2.25 - 12.90) ไม่พบไขมันเป็นส่วนประกอบภายในก้อน (OR, 46.50; 95% CI, 5.25 - 411.90) และตำแหน่งของก้อนจะอยู่ทางด้านนอก (OR, 7.41; 95% CI, 1.63 - 33.73) และร่วมกันทั้งด้านนอกและด้านใน (OR, 26.22; 95% CI, 4.23 - 162.58) โดยมีความเห็นสอดคล้องตรงกันระหว่างรังสีแพทย์อยู่ในระดับปานกลางถึงระดับมาก (κ = 0.43 - 0.91)

สรุป: ลักษณะก้อนเดี่ยวในไตจากภาพเอกซเรย์คอมพิวเตอร์ที่ไม่พบไขมันเป็นส่วนประกอบ เป็นลักษณะทางรังสีที่สำคัญที่สุดในการแยกมะเร็งไตชนิดเซลล์เนื้อเยื่อไต ออกจากพยาธิสภาพอื่น

คำสำคัญ: มะเร็งไตชนิดชนิดเซลล์เนื้อเยื่อไต ก้อนที่ไต เอกซเรย์คอมพิวเตอร์

Rama Med J: doi:10.33165/rmj.2020.43.1.176267

Received: May 22, 2019 **Revised:** October 29, 2019 **Accepted:** February 6, 2020

Corresponding Author:
พรพรรณ วิบุลผลประเสริฐ
ภาควิชารังสีวิทยา
คณะแพทยศาสตร์
โรงพยาบาลรามาธิบดี
มหาวิทยาลัยมหิดล
270 ถนนพระรามที่ 6
แขวงทุ่งพญาไท เขตราชเทวี
กรุงเทพฯ 10400 ประเทศไทย
โทรศัพท์ +66 2201 1212
โทรสาร +66 2201 1297
อีเมล punlee77@gmail.com,
pornphan.wib@mahidol.ac.th